



## Article

# Functional Characterization of Arylalkylamine *N*-Acetyltransferase, a Pivotal Gene in Antioxidant Melatonin Biosynthesis from *Chlamydomonas reinhardtii*

Ok-Jin Hwang and Kyounghwan Back \*

Department of Biotechnology, College of Agriculture and Life Sciences, Chonnam National University, Gwangju 61186, Korea

\* Correspondence: kback@chonnam.ac.kr; Tel.: +82-62-530-2165

**Abstract:** Arylalkylamine *N*-acetyltransferase (AANAT) is a pivotal enzyme in melatonin biosynthesis that catalyzes the conversion of serotonin to *N*-acetylserotonin. Homologs of animal AANAT genes are present in animals, but not in plants. An AANAT homolog was found in *Chlamydomonas reinhardtii*, but not other green algae. The characteristics of *C. reinhardtii* AANAT (*CrAANAT*) are unclear. Here, full-length *CrAANAT* was chemically synthesized and expressed in *Escherichia coli*. Recombinant *CrAANAT* exhibited AANAT activity with a  $K_m$  of 247  $\mu$ M and  $V_{max}$  of 325 pmol/min/mg protein with serotonin as the substrate. *CrAANAT* was localized to the cytoplasm in tobacco leaf cells. Transgenic rice plants overexpressing *CrAANAT* (*CrAANAT*-OE) exhibited increased melatonin production. *CrAANAT*-OE plants showed a longer seed length and larger second leaf angle than wild-type plants, indicative of the involvement of brassinosteroids (BRs). As expected, BR biosynthesis- and signaling-related genes such as *D2*, *DWARF4*, *DWARF11*, and *BZR1* were upregulated in *CrAANAT*-OE plants. Therefore, an increased endogenous melatonin level by ectopic overexpression of *CrAANAT* seems to be closely associated with BR biosynthesis, thereby influencing seed size.

**Keywords:** brassinosteroids; cytokinin; green algae; melatonin; seed size; serotonin *N*-acetyltransferase; transgenic rice



**Citation:** Hwang, O.-J.; Back, K. Functional Characterization of Arylalkylamine *N*-Acetyltransferase, a Pivotal Gene in Antioxidant Melatonin Biosynthesis from *Chlamydomonas reinhardtii*. *Antioxidants* **2022**, *11*, 1531. <https://doi.org/10.3390/antiox11081531>

Academic Editors: Mohsin Tanveer, Zhong-Hua Chen, Yizhou Wang and Ricardo Aroca

Received: 13 July 2022

Accepted: 3 August 2022

Published: 5 August 2022

**Publisher's Note:** MDPI stays neutral with regard to jurisdictional claims in published maps and institutional affiliations.



**Copyright:** © 2022 by the authors. Licensee MDPI, Basel, Switzerland. This article is an open access article distributed under the terms and conditions of the Creative Commons Attribution (CC BY) license (<https://creativecommons.org/licenses/by/4.0/>).

## 1. Introduction

Arylalkylamine *N*-acetyltransferase (AANAT) is the penultimate enzyme for melatonin biosynthesis in animals and plants. It catalyzes the conversion of serotonin to *N*-acetylserotonin, which is the substrate for melatonin synthesis by *N*-acetylserotonin *O*-methyltransferase (ASMT) [1,2]. AANAT is also named serotonin *N*-acetyltransferase (SNAT); therefore, to differentiate them from animal AANAT genes, plant AANAT genes are frequently termed SNAT genes. Both animal AANAT and plant SNAT proteins belong to the GCN5-related *N*-acetyltransferase superfamily, which transfer an acetyl group from acetyl-coenzyme A (CoA) [3]. However, there is no significant amino sequence homology between animal AANATs and plant SNATs except for a few amino acids in the acetyl-CoA-binding domain [4]. Interestingly, an animal homolog of arylalkylamine *N*-acetyltransferase (AANAT) is present in the genome of *C. reinhardtii*, but not in other green algae or higher plants [3,5,6].

Based on the key role of AANAT (or SNAT) in melatonin biosynthesis, many animal AANAT and plant SNAT genes have been cloned and their recombinant proteins functionally characterized in vitro [7,8]. Ectopic overexpression of animal AANAT or plant SNAT genes in plant species resulted in increased melatonin synthesis [9,10]. The resulting AANAT- or SNAT-overexpressing transgenic plants exhibited increased melatonin synthesis and enhanced responses to biotic and abiotic stresses, including ultraviolet-B [11], high temperature [12], pathogen [13], salt [14], high light [15], cadmium [16,17], drought [18], oxidative stress [19], and cold exposure [20]. The enhanced tolerance to various stresses

in AANAT- or SNAT-overexpressing plants was attributable to melatonin overproduction because melatonin not only has antioxidant activity but also induces antioxidant enzymes such as catalase, peroxidase, and superoxide dismutase [9,21].

CrAANAT was first characterized by Okazaki et al. [22]. CrAANAT transfers an acetyl group to serotonin. Transgenic tomato plants overexpressing CrAANAT had an increased melatonin level. However, the  $K_m$  and  $V_{max}$  values of recombinant CrAANAT and the phenotypes of CrAANAT-overexpressing transgenic plants are unknown. The aim of this work was to determine the enzyme kinetics of CrAANAT and its functional role in melatonin biosynthesis through heterologous expression in rice genome. We purified recombinant CrAANAT and determined the  $K_m$  and  $V_{max}$  values of its AANAT activity. Ectopic overexpression of CrAANAT in the rice genome increased the seed length and upregulated brassinosteroid (BR) (rather than cytokinin)-related gene expression.

## 2. Materials and Methods

### 2.1. Synthesis of *C. reinhardtii* AANAT

Based on AANAT of *C. reinhardtii* (CrAANAT; GenBank accession AB474787), the 192 codons of CrAANAT (including the stop codon) were manually optimized according to SNAT2 codons of rice [23]. Codon-optimized synthetic CrAANAT was custom-synthesized by Bioneer (Daejeon, South Korea).

### 2.2. Affinity Purification of Various Recombinant *C. reinhardtii* AANAT Proteins from *Escherichia coli* Expression

Four different types of *Escherichia coli* vectors were employed to express the full-length synthetic *Chlamydomonas reinhardtii* AANAT (CrAANAT) DNA. Two vectors were pET300 (Invitrogen, Carlsbad, CA, USA) and pET28b (Novagen, San Diego, CA, USA) which are designed to express the CrAANAT in either N-terminal- or C-terminal- hexahistidine tagged form. The other two vectors were pET32b (Novagen) and pET60 (Novagen) which are designed to express the CrAANAT in N-terminal fusion proteins of either thioredoxin (Trx) or glutathione-s-transferase (GST). As for pET300, CrAANAT-attB1 forward primer (5'-AAA AAG CAG GCT CCA TGG CTG AGG AGT CGC-3') and CrAANAT-attB2 reverse primer (5'-AGA AAG CTG GGT CTA GGC CTC AGC AGC CTC-3') were used for PCR amplification with the synthetic CrAANAT gene followed by second PCR using adaptor primers with attB recombination sequences (attB1 adaptor forward primer, 5'-GGG GAC AAG TTT GTA CAA AAA AGC AGG CT-3'; attB2 adaptor reverse primer, 5'-GGG GAC CAC TTT GTA CAA GAA AGC TGG GT-3'). The resulting PCR product was gel purified and cloned into the pDONR221 Gateway<sup>®</sup> vector (Invitrogen) via BP (between the attB and the attP sites) recombination. The pDONR221:CrAANAT gene entry vector was then recombined with the pET300 Gateway destination vector via LR (between the attL and the attR sites) recombination to form the pET300-CrAANAT vector. A pET28b-CrAANAT was constructed by PCR with NcoI forward primer (5'-ACC ATG GCT GAG GAG TCG CTC-3') and XhoI reverse primer (5'-CTC GAG GGC CTC AGC AGC CTC TGC-3'). To generate pET60-CrAANAT, the CrAANAT-attB1 forward primer and 6×His attB2 reverse primer (5'-AGA AAG CTG GGT TCA GTG GTG GTG GTG GTG-3') were used to amplify the CrAANAT with the pET28b-CrAANAT plasmid as a template. The resulting PCR product was further amplified with the attB1 adaptor forward and attB2 adaptor reverse primers followed by BP and LR recombination reactions as described above. A pET32b-CrAANAT was constructed by ligating the NcoI and XhoI insert prepared during the pET28b-CrAANAT vector construction. All plasmids were transformed into *E. coli* strain BL21(DE3) (Novagen).

### 2.3. Purification of Recombinant CrAANAT Proteins

Each 10 mL of *E. coli* overnight culture of *E. coli* containing pET300-CrAANAT, pET28b-CrAANAT, pET60-CrAANAT, and pET32b-CrAANAT plasmid vectors was inoculated into 100 mL of Terrific Broth (20 g/L Bacto-tryptone, 24 g/L Bacto-yeast extract, 4 mL/L glycerol,

and phosphate buffer [0.017 M monopotassium phosphate and 0.072 M dipotassium phosphate] containing with 50 mg/L ampicillin or 50 mg/L kanamycin (pET28b-CrAANAT) and incubated at 37 °C until the optical density at 600 nm reached 1.0 about 3 to 4 h. The culture was added with 1 mM isopropyl- $\beta$ -D-thiogalactopyranoside (Sigma, St. Louis, MO, USA) and grown at 28 °C with shaking at 180 rpm for 5 h. The protein was purified via affinity nickel ion chromatography according to the column manufacturer's instructions (Qiagen, Tokyo, Japan).

#### 2.4. Measurement of Serotonin N-Acetyltransferase (SNAT) Enzyme Activity

Two types of purified recombinant CrAANAT proteins were incubated in 100  $\mu$ L of 100 mM potassium phosphate (pH 8.8 or various pH values) in the presence of 0.5 mM serotonin and 0.5 mM acetyl-coenzyme A. SNAT enzyme assays were conducted at 45 °C for 30 min (or various temperatures) and stopped by adding 25  $\mu$ L of methanol. Then, 10  $\mu$ L aliquots of the reaction mixture were subjected to high-performance liquid chromatography (HPLC) coupled to a fluorescence detector system to detect *N*-acetylserotonin as described previously [24]. Non-enzymatic reaction products that were generated without the CrAANAT enzymes were deducted. To acquire substrate affinity ( $K_m$ ) and maximum reaction rate ( $V_{max}$ ), various substrates (50 to 2000  $\mu$ M serotonin) and enzyme concentrations (0.2 to 1  $\mu$ g) were employed. The  $K_m$  and  $V_{max}$  values were calculated using Lineweaver–Burk plots. Protein concentration was determined using Bradford assays (Bio-Rad, Hercules, CA, USA). The analyses were performed in triplicate.

#### 2.5. Subcellular Localization of CrAANAT

The pER-mCherry vector which was kindly donated by Dr. H. Kang (Texas State University, San Marcos, TX, USA) was used for assessing the localization of CrAANAT protein in tobacco leaves. Full-length *CrAANAT* cDNA was amplified by PCR with two *AscI* containing primers (*CrAANAT AscI* forward primer 5'-GGC GCG CCA TGG CTG AGG AGT CGC TCG-3'; *CrAANAT AscI* reverse primer 5'-GGC GCG CCG GGC CTC AGC AGC CTC TGC-3'). The resulting PCR product was first cloned into the T&A cloning vector (T&A:CrAANAT; RBC Bioscience, New Taipei City, Taiwan) from which the *AscI* insert of CrAANAT was produced and cloned into the binary pER8-mCherry vector at the *AscI* restriction sites downstream of the estrogen-inducible XVE promoter to generate CrAANAT-mCherry fusion proteins. The plasmid was transformed into *Agrobacterium tumefaciens* strain GV2260 using the freeze-thaw method. As for a transient expression analysis of CrAANAT-mCherry, the leaves of two-week-old tobacco (*Nicotiana benthamiana*) plant, a native Australian species, were infiltrated with *A. tumefaciens* strain GV2260 carrying pER8:CrAANAT-mCherry plasmid. The transformed tobacco leaves were then examined using confocal microscopy to determine the subcellular localization of the CrAANAT-mCherry fusion proteins. Further treatment with  $\beta$ -estradiol (Sigma Aldrich, St. Louis, MO, USA) and confocal microscopy analysis were described previously [24].

#### 2.6. Vector Construction and Production of CrAANAT-Overexpressing Transgenic Rice Plants

The pDONR221:CrAANAT gene entry vector harboring the synthetic *CrAANAT* gene was then recombined with the pIPKb002 destination vector [25] via LR recombination to yield pIPKb002-CrAANAT, which was transformed into *Agrobacterium tumefaciens* strain LBA4404. We used *Agrobacterium*-mediated rice transformation with the coculture with rice scutellum-derived calli to generate transgenic rice (*Oryza sativa* cv. Dongjin, a Korean *japonica* cultivar) plants as described previously [26].

#### 2.7. Plant Growth Conditions

Rice (*Oryza sativa* cv. Dongjin, a Korean *japonica* cultivar) seeds of both wild type and *CrAANAT* overexpression (*CrAANAT*-OE) were sterilized with 2% sodium hypochlorite and rinsed with sterile distilled water. Sterilized seeds were grown on half-strength Murashige and Skoog (MS) medium under cool daylight fluorescent lamps (60  $\mu$ mol m<sup>-2</sup> s<sup>-1</sup>)

(Philips, Amsterdam, Netherlands) in 14-h light/10-h dark photoperiod at 28 °C/24 °C (day/night) for 7 days. Germinated seeds were grown in a paddy field at the Chonnam National University (35°09' N and 126°54' W; 53 m a.s.l), Gwangju, Korea in 2021. The distance between the rice plants within a row was 30 cm, and the distance between the rows was 30 cm. Grain length, grain width and 1000-grain weight were measured after harvesting followed by drying for 1 month at room temperature of about 26 °C.

### 2.8. Chemical Treatment

Seven-day-old rice seedlings were incubated in 30 mL of 100 µM 5-methoxytryptamine (Sigma-Aldrich, St. Louis, MO, USA) dissolved in 0.02% ethanol for 1 day under cool daylight fluorescent lamps (60 µmol m<sup>-2</sup> s<sup>-1</sup>) (Philips) in 14-h light/10-h dark photoperiod at 28 °C/24 °C (day/night). The 0.02% ethanol was used as a control. The leaves and stems were harvested for further analyses.

### 2.9. Quantitative Real Time-Polymerase Chain Reaction (qRT-PCR) Analysis

Total RNA from rice plants was isolated using a NucleoSpin RNA Plant Kit (Macherey-Nagel, Düren, Germany). First-strand cDNA was synthesized from 2 µg of total RNA using EcoDry™ Premix (Takara Bio USA, Inc., Mountain View, CA, USA). qRT-PCR was performed in a Mic qPCR Cycler system (Biomolecular Systems, Queensland, VIC, Australia) with specific primers and the TB Green® Premix Ex Taq™ (Takara Bio Inc., Kusatsu, Shiga, Japan). The expression of genes was analyzed using Mic's RQ software v2.2 (Biomolecular Systems) and normalized to *actin 1* (*ACT1*). Reverse transcription (RT)-PCR and quantitative real-time (qRT)-PCR were performed with the primer set (Table S1).

### 2.10. Quantification of Melatonin

Frozen samples (0.1 g) were ground in liquid nitrogen with the use of the TissueLyser II (Qiagen, Tokyo, Japan) and extracted with 1 mL of chloroform. The chloroform extracts were centrifuged for 10 min at 12,000 × g, and the supernatants (200 µL) were completely evaporated and dissolved in 0.1 mL of 40% methanol, and 20-µL aliquots were subjected to HPLC using a fluorescence detector system (Waters, Milford, MA, USA) as described previously [27]. In brief, melatonin was detected at 280 nm (excitation) and 348 nm (emission) on a Sunfire C18 column (Waters 4.6 × 150 mm) in the following gradient elution condition: from 42% to 50% methanol in 0.1% formic acid for 27 min, followed by isocratic elution with 50% methanol in 0.1% formic acid for 18 min at a flow rate of 0.15 mL/min. All measurements were performed in triplicate.

### 2.11. Statistical Analyses

The data were analyzed using analysis of variance (ANOVA) using IBM SPSS Statistics 23 software (IBM Corp., Armonk, NY, USA). Means with asterisks indicate significantly different values at  $p < 0.05$ , according to a Fisher's least significant difference (LSD) test. All data are presented as mean ± standard deviations.

## 3. Results

### 3.1. Codon-Optimized Synthesis of CrAANAT and Its Expression in *Escherichia coli*

The full-length CrAANAT nucleotide sequence (encoding 191 amino acids) was chemically synthesized based on the codon usage of rice SNAT2 (AK068156) exhibiting a 70% G+C content. Among the 192 codons of CrAANAT, 55 were modified in the synthetic CrAANAT gene, increasing the G+C content from 64% to 67% (Figures 1 and 2).

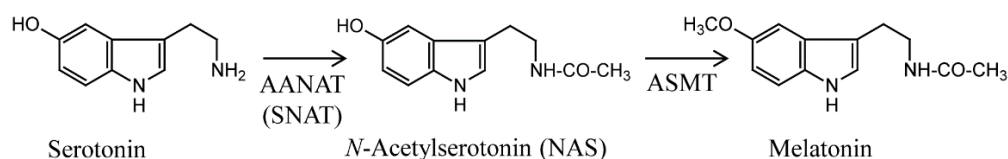


**Figure 1.** Schematic diagram of melatonin biosynthesis. AANAT is also known as serotonin *N*-acetyltransferase (SNAT) in plants. ASMT, *N*-acetylserotonin *O*-methyltransferase.

Native	1	ATG	GCC	GAG	GAA	TCT	CTA	GAC	GCC	AGT	GTA	CAG	CCA	CTA	39
Synthetic	1	---	---	---	---	---	---	---	---	---	---	---	---	---	39
		Met	Ala	Glu	Glu	Ser	Leu	Asp	Ala	Ser	Val	Gln	Pro	Leu	
Native	40	GGC	TCT	ACC	GTT	TTC	TTT	GGC	CCG	GTG	CAG	CCA	GAG	ATG	78
Synthetic	40	---	---	---	---	---	---	---	---	---	---	---	---	---	78
		Gly	Ser	Thr	Val	Phe	Phe	Gly	Pro	Val	Gln	Pro	Glu	Met	
Native	79	CTG	GAC	CGA	ATT	CAT	GAA	CTT	GAA	GCT	GCC	TCT	TAC	CCA	117
Synthetic	79	---	---	---	---	---	---	---	---	---	---	---	---	---	117
		Leu	Asp	Arg	Ile	His	Glu	Leu	Glu	Ala	Ala	Ser	Tyr	Pro	
Native	118	GAA	GAC	GAG	GCC	GCT	ACT	TAC	GAG	AAG	CTA	AAG	TTC	AGG	156
Synthetic	118	---	---	---	---	---	---	---	---	---	---	---	---	---	156
		Glu	Asp	Glu	Ala	Ala	Thr	Tyr	Glu	Lys	Leu	Lys	Phe	Arg	
Native	157	ATC	GAA	AAC	GCG	TCG	AAC	GTG	TTC	CTG	GTC	GCG	CTG	TCG	195
Synthetic	157	---	---	---	---	---	---	---	---	---	---	---	---	---	195
		Ile	Glu	Asn	Ala	Ser	Asn	Val	Phe	Leu	Val	Ala	Leu	Ser	
Native	196	GCG	GAG	GGC	GAC	GGG	GAG	CCC	AAG	GTC	GTC	GGG	TTT	GTG	234
Synthetic	196	---	---	---	---	---	---	---	---	---	---	---	---	---	234
		Ala	Glu	Gly	Asp	Gly	Glu	Pro	Lys	Val	Val	Gly	Phe	Val	
Native	235	TGC	GGC	ACG	CAA	ACG	CGC	GCG	TCT	AAG	CTG	ACA	CAC	GAG	273
Synthetic	235	---	---	---	---	---	---	---	---	---	---	---	---	---	273
		Cys	Gly	Thr	Gln	Thr	Arg	Ala	Ser	Lys	Leu	Thr	His	Glu	
Native	274	TCC	ATG	TCA	ACG	CAC	GAT	GCC	GAC	GGC	GCA	CTA	CTG	TGC	312
Synthetic	274	---	---	---	---	---	---	---	---	---	---	---	---	---	312
		Ser	Met	Ser	Thr	His	Asp	Ala	Asp	Gly	Ala	Leu	Leu	Cys	
Native	350	ATC	CAC	TCG	GTG	GTG	GTG	GAC	GCC	GCG	CTG	CGC	CGG	CGC	351
Synthetic	350	---	---	---	---	---	---	---	---	---	---	---	---	---	351
		Ile	His	Ser	Val	Val	Val	Asp	Ala	Ala	Leu	Arg	Arg	Arg	
Native	352	GGC	CTG	GCC	ACC	CGC	ATG	CTC	CGA	GCC	TAC	ACC	GCC	TTC	390
Synthetic	352	---	---	---	---	---	---	---	---	---	---	---	---	---	390
		Gly	Leu	Ala	Thr	Arg	Met	Leu	Arg	Ala	Tyr	Thr	Ala	Phe	
Native	391	GTG	GCC	GCC	ACC	TCC	CCG	GGC	CTG	ACC	GGG	ATA	CGG	CTG	429
Synthetic	391	---	---	---	---	---	---	---	---	---	---	---	---	---	429
		Val	Ala	Ala	Thr	Ser	Pro	Gly	Leu	Thr	Gly	Ile	Arg	Leu	
Native	430	CTG	ACC	AAG	CAG	AAC	CTG	ATC	CCG	CTG	TAC	GAG	GGC	GCG	468
Synthetic	430	---	---	---	---	---	---	---	---	---	---	---	---	---	468
		Leu	Thr	Lys	Gln	Asn	Leu	Ile	Pro	Leu	Tyr	Glu	Gly	Ala	
Native	469	GGC	TTC	ACT	CTG	CTT	GGC	CCC	TCG	GAC	GTC	GAG	CAC	GGC	507
Synthetic	469	---	---	---	---	---	---	---	---	---	---	---	---	---	507
		Gly	Phe	Thr	Leu	Leu	Gly	Pro	Ser	Asp	Val	Glu	His	Gly	
Native	508	GCC	GAC	CTG	TGG	TAC	GAA	TGC	GCC	ATG	GAG	CTG	GAG	GCG	546
Synthetic	508	---	---	---	---	---	---	---	---	---	---	---	---	---	546
		Ala	Glu	Leu	Trp	Tyr	Glu	Cys	Ala	Met	Glu	Leu	Glu	Ala	
Native	547	GAG	GAG	GAG	GCG	GAG	GCG	GCG	GAA	GCC	TAG				576
Synthetic	547	---	---	---	---	---	---	---	---	---	---				576
		Glu	Glu	Glu	Ala	Glu	Ala	Ala	Glu	Ala					

**Figure 2.** Nucleotide sequence alignments of native (black writing; AB474787) and synthetic *CrAANAT* (red writing) genes. Identity is denoted by red dashes. The nucleotide sequence of synthetic *CrAANAT* was codon-optimized with reference to rice *SNAT2* (AK068156).

Synthetic *CrAANAT* was expressed in *E. coli* as a fusion protein with an N- or C-terminal hexa-histidine (His6) tag, followed by Ni<sup>2+</sup> affinity purification (Figure 3). Intact His6-*CrAANAT* and *CrAANAT*-His6 were insoluble and so could not be purified using a Ni<sup>2+</sup> affinity column. However, *CrAANAT* fusions with thioredoxin (Trx) or glutathione-s-transferase (GST) were soluble and subjected to Ni<sup>2+</sup> affinity purification (Figure 3A,B). Recombinant Trx-*CrAANAT*-His6 exhibited serotonin *N*-acetyltransferase (SNAT) activity of 10.1 pkat/mg protein at 45 °C and pH 8.8, compared to 18.7 pkat/mg protein for GST-*CrAANAT*-His6 (Figure 3C). Therefore, *CrAANAT* transfers an acetyl

group from acetyl-CoA to serotonin to produce *N*-acetylserotonin, the final substrate in melatonin biosynthesis [4].

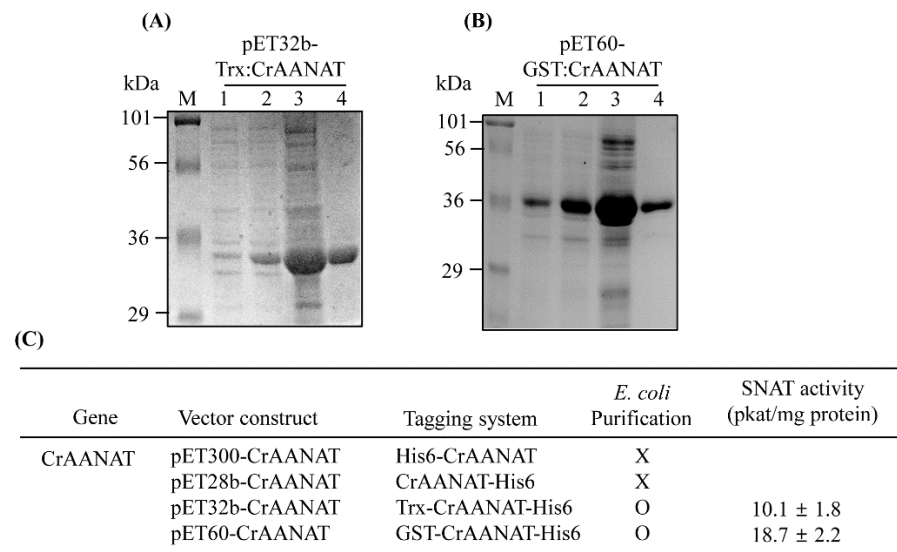


**Figure 3.** Expression of *CrAANATs* in *Escherichia coli*. (A) Affinity purification of thioredoxin (Trx)-*CrAANAT*. (B) Affinity purification of glutathione-s-transferase (GST)-*CrAANAT*. (C) SNAT activity of purified recombinant *CrAANAT*. Protein samples were separated by SDS-PAGE and stained with Coomassie brilliant blue. M, molecular size standard; 1, total proteins in 10  $\mu$ L aliquots of bacterial cell culture without isopropyl  $\beta$ -D-thiogalactopyranoside (IPTG); 2, total proteins after IPTG treatment; 3, 20  $\mu$ g of soluble protein extract from supernatant after centrifugation at  $15,000\times g$ ; 4, recombinant proteins purified by affinity (Ni-NTA) chromatography. X, no purification; O, successful purification.

### 3.2. Kinetics of Recombinant *CrAANAT*

SNAT activity peaked at pH 8.8 and was similar at pH 7.8 (Figure 4). This high pH optimum is consistent with that of other plant SNAT proteins [8,13,23,28,29] but unlike animal AANAT proteins (pH 6.7) [30,31]. SNAT activity was fourfold lower at pH 6.5 than at pH 8.8. SNAT activity was highest at 45  $^{\circ}$ C followed by 37  $^{\circ}$ C. The high level of SNAT activity at 37  $^{\circ}$ C is similar to other animal AANAT proteins but not plant SNAT proteins [8,30,31]. The  $K_m$  and  $V_{max}$  values were 247  $\mu$ M and 5.4 pkat/mg protein (325 pmol/min/mg protein), respectively. The  $K_m$  value of *CrAANAT* is similar to those of rice [24], Arabidopsis [29], and tobacco [8], but lower than that of red algae [32] and cyanobacteria [33]. The  $K_m$  value of *CrAANAT* was threefold higher than that of sheep AANAT [7]. In contrast, the  $V_{max}$  value of *CrAANAT* was lower than that of plant SNATs and sheep AANATs. Therefore, the kinetics of *CrAANAT* has similarities to those of plant SNATs and animal AANATs. To be more precise, the *CrAANAT* is close to plant SNAT at the level of  $K_m$  value, but to animal AANAT at the level of  $V_{max}$  value.

### 3.3. Subcellular Localization of *CrAANAT*

Because in silico TargetP analysis of *CrAANAT* showed no transit or signal sequence [34], we hypothesized that *CrAANAT* is cytoplasmic. We subcloned *CrAANAT* into a binary vector to express the *CrAANAT*-mCherry fusion protein under the control of the estrogen-inducible XVE promoter. *Agrobacterium* cells harboring the binary vector were infiltrated into tobacco leaves followed by transgene induction by  $\beta$ -estradiol. Confocal microscopy showed that *CrAANAT*-mCherry exhibited strong mCherry fluorescence, which co-localized with the green fluorescence of cytoplasmic GFP (Figure 5). Therefore, *CrAANAT* localizes to the cytoplasm, as does sheep AANAT [35]. *CrAANAT* in the cytoplasm is unlike the chloroplastic localizations of other plant SNAT proteins [8,13,24].

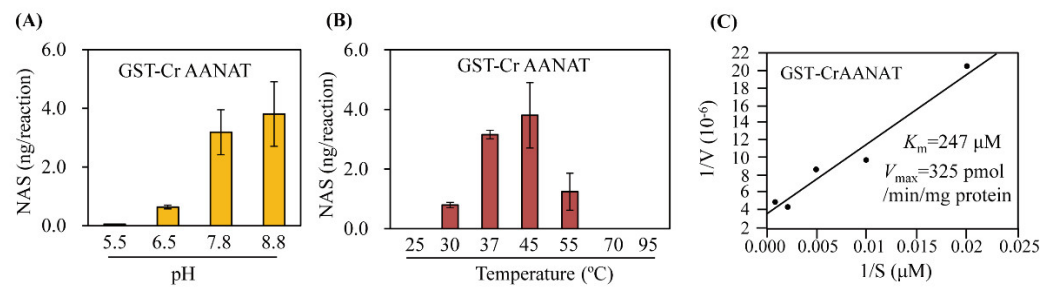


**Figure 4.** Conversion of serotonin to *N*-acetylserotonin as a function of (A) pH and (B) temperature. (C) Substrate affinity ( $K_m$ ) and maximum reaction rate ( $V_{\text{max}}$ ) values of CrAANAT. Purified recombinant GST-CrAANAT (1  $\mu\text{g}$ ) was incubated at a range of pH values and temperatures for 30 min.  $K_m$  and  $V_{\text{max}}$  values were determined using Lineweaver-Burk plots. *N*-Acetylserotonin, an in vitro enzymatic product, was quantified by high-performance liquid chromatography. The data are means  $\pm$  standard deviation ( $n = 3$ ).

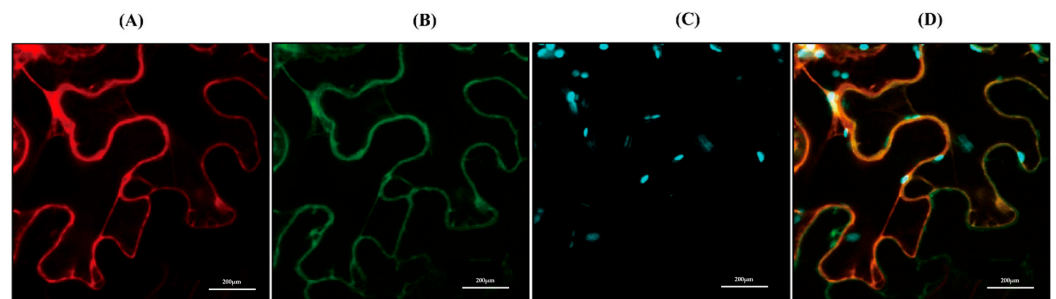


**Figure 5.** Localization of CrAANAT. (A) Red fluorescence of CrAANAT-mCherry. (B) Green fluorescence of cytoplasmic GFP. (C) Cyan fluorescence of chloroplasts. (D) Merged image (A + B + C). Leaves of 30-day-old tobacco (*Nicotiana benthamiana*) seedlings were infiltrated with *Agrobacterium* (GV2260) containing XVE-inducible CrAANAT-mCherry, or constitutive 35S:GFP (cytosolic marker). Bars, 20  $\mu\text{m}$ . Synthetic CrAANAT was used in place of native CrAANAT (AB474787).

### 3.4. Transgenic Rice Plants Overexpressing CrAANAT (CrAANAT-OE)

To determine whether CrAANAT is functionally coupled to melatonin biosynthesis in vivo, we generated CrAANAT-OE under the control of the maize ubiquitin promoter (Figure 6A).

Six homozygous T<sub>2</sub> CrAANAT-OE were selected from 11 independent T<sub>1</sub> transgenic rice seeds (Figure 6A,B). These T<sub>2</sub> CrAANAT-OE showed CrAANAT overexpression whereas CrAANAT transcript was not detected in wild type (WT). The T<sub>2</sub> homozygous CrAANAT-OE, particularly line 7, showed slightly increased seedling growth (Figure 6C,D). When these T<sub>2</sub> homozygous transgenic seedlings were rhizospherically challenged for 24 h with 100  $\mu\text{M}$  5-methoxytryptamine (5-MT), a substrate for AANAT-catalyzed melatonin biosynthesis, the WT and CrAANAT-OE lines produced 83 and 116 ng/g fresh weight (FW) (Figure 6E). Therefore, CrAANAT converts 5-MT into melatonin by acetylating 5-MT, as do most animal AANAT and plant SNAT proteins [8,36]. In the absence of 5-MT, the WT and CrAANAT-OE lines produced melatonin at 0.2 and 0.45 ng/g FW (Figure 6F). Therefore, ectopic overexpression of CrAANAT increased AANAT activity compared to wild type. CrAANAT overexpression was functionally associated with enhanced production of melatonin in the CrAANAT-OE line compared to wild type.

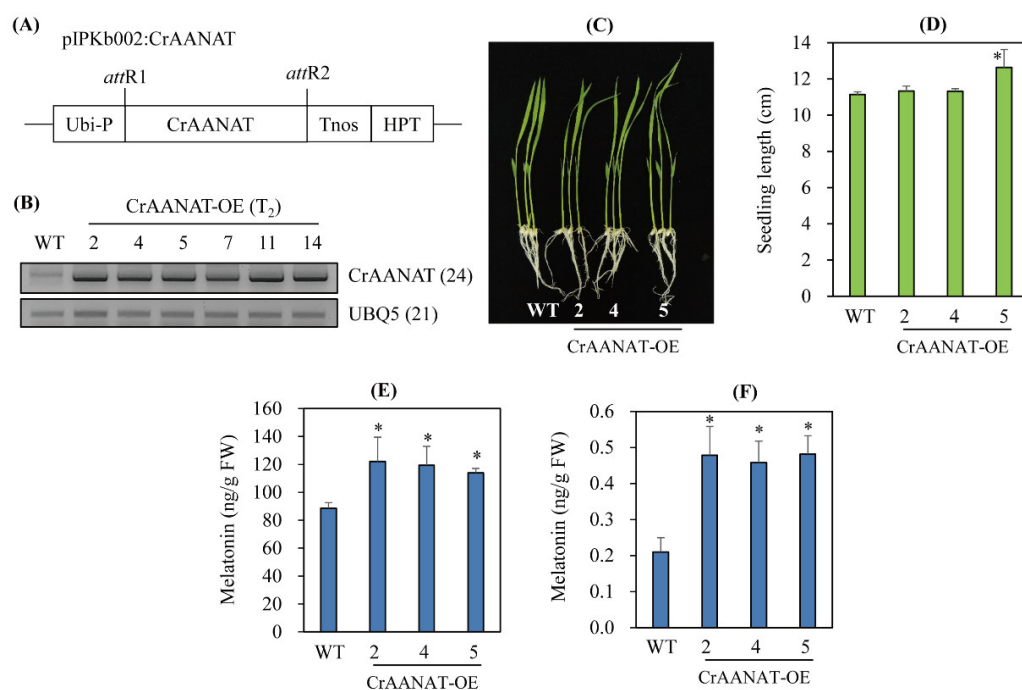


**Figure 6.** Structure of the pIPKb002-CrAANAT binary vector and its overexpression in transgenic rice plants. (A) Schematic diagram of the pIPKb002:CrAANAT binary vector. (B) Expression of *CrAANAT* in wild type (WT) and *CrAANAT*-overexpressing (*CrAANAT*-OE) seedlings (T<sub>2</sub>). (C) Phenotypes of 7-day-old rice seedlings of WT and *CrAANAT*-OE transgenic plants (T<sub>2</sub>). (D) Seedling lengths of WT and *CrAANAT*-OE plants. (E) Melatonin contents in 7-day-old rice seedlings after 100  $\mu$ M 5-methoxytryptamine (5-MT) in 0.02% ethanol. (F) Melatonin contents in 7-day-old rice seedlings after 0.02% ethanol treatment. Seven-day-old rice seedlings were rhizospherically challenged with 100  $\mu$ M 5-MT for 24 h in 0.02% ethanol. \*, significant difference from wild type ( $p < 0.05$ ; ANOVA, followed by Fisher's LSD test). The numbers of PCR cycles are shown in parentheses. Synthetic *CrAANAT* was overexpressed in the rice genome. *Ubi-P*, maize ubiquitin promoter; *HPT*, hygromycin phosphotransferase; *Tnos*, nopaline synthase terminator. GenBank accession number of *UBQ5*, Os03g13170.

Homozygous T<sub>2</sub> *CrAANAT*-OE seeds were of greater length, but lesser width, than WT seeds (Figure 7). The 1000-seed weight was similar in the *CrAANAT*-OE lines and wild type. To determine whether the increase in seed length is associated with BRs, we measured the second leaf angle, a phenotypic marker of BR levels. The second-leaf angle was larger in the *CrAANAT*-OE seedlings than in WT seedlings (Figure 8A), indicating increased BR levels. Cytokinins also regulate seed size in plants [37]. To identify the hormones responsible for the increased seed length in the *CrAANAT*-OE lines, we evaluated the expression levels of BR- and cytokinin-related genes. The expression levels of BR-related genes were significantly increased in the *CrAANAT*-OE lines (the BR biosynthesis-related genes *DWARF [D]2*, *D4*, and *D11* and *BRASSINOZOLE-RESISTANT 1 (BZR1)*, encoding a transcription factor that regulates BR-responsive gene expression; Figure 8B) [38,39]. By contrast, cytokinin degradation genes (*CKX2*, *CKX4*, and *CKX10*) and cytokinin biosynthesis genes (*LOGL1*, *LOGL3*, and *LOGL10*) were upregulated. Therefore, the increased lamina angle and seed length in the *CrAANAT*-OE line compared to wild type are caused by BRs rather than cytokinins.

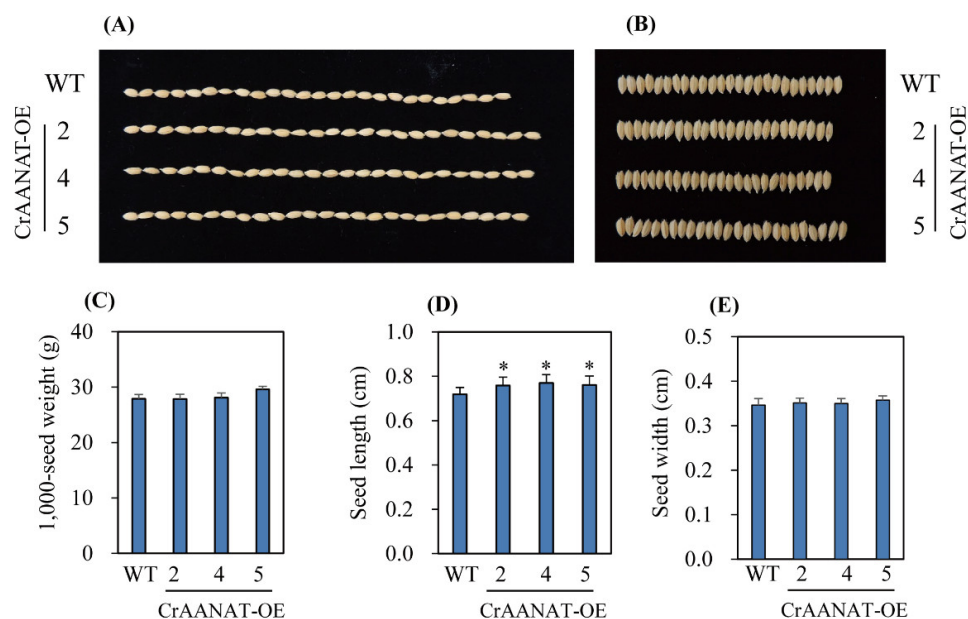


**Figure 7.** Morphology of  $T_2$  homozygous transgenic *CrAANAT*-OE seeds. (A) Photograph of WT and *CrAANAT*-OE seeds ( $T_2$ ). (B) Photograph of WT and *CrAANAT*-OE seeds ( $T_2$ ). (C) The weight of 1000 seeds of WT and *CrAANAT*-OE transgenic rice ( $T_2$ ). (D) Seed length. (E) Seed width. \* Significant difference from wild type ( $p < 0.05$ ; Fisher's LSD test).

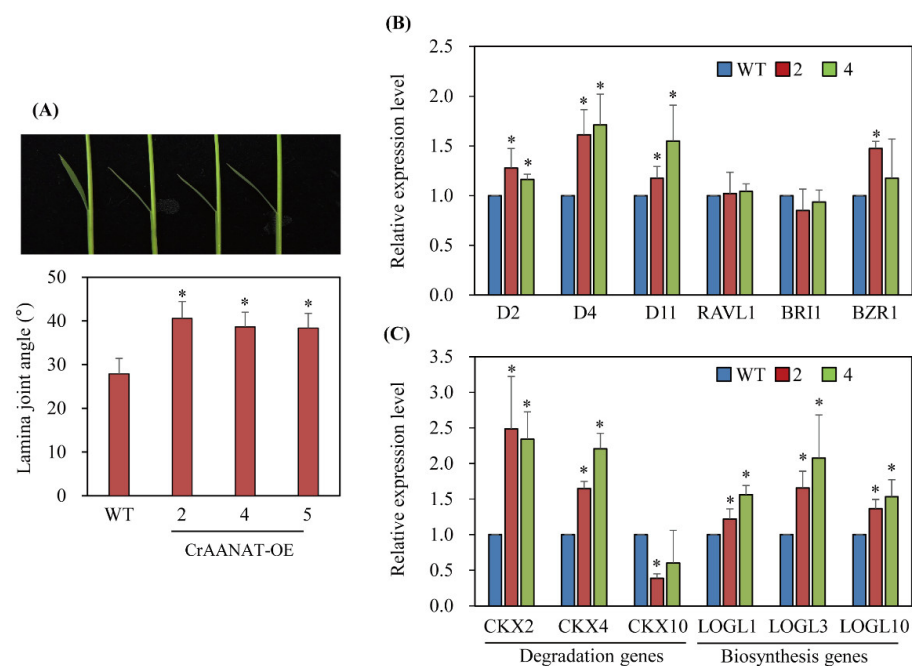


**Figure 8.** Second-leaf angle and cytokinin and brassinosteroid (BR) biosynthesis-related gene expression. (A) Second-leaf angle. (B) Quantitative real-time (qRT)-PCR of BR biosynthesis- and signaling-related genes. (C) qRT-PCR of cytokinin biosynthesis- and degradation-related genes. Fourteen-day-old rice seedlings grown in soil were used to measure the lamina angle of the second leaf; meristem parts of rice seedlings, including second leaves, were subjected to total RNA extraction and qRT-PCR. GenBank accession numbers are *CKX2*, cytokinin oxidase2 (Os01g0197700); *CKX4* (Os01g0940000); *CKX10* (Os06g0572300); *LOGL1*, LONELY GUY LIKE phosphoribohydrolase1 (Os01g0708500); *LOGL3* (Os03g0109300); *LOGL10* (Os10g0479500); *D2*, DWARF2 (XP-015611433); *D4*, DWARF4 (AB206579); *D11*, DWARF11 (AK106528); *RAVL1*, RAV Like1 (Os04g0581400); *BRI1* (AK101085); *BZR1* (Os07g39220); *ACT1* (Os03g50885). \* Significant difference from wild type ( $p < 0.05$ ; Fisher's LSD test).

#### 4. Discussion

The final two genes in melatonin biosynthesis are *AANAT* (or *SNAT*) and *ASMT* [4]. *AANAT* was first cloned and characterized in sheep and rats [40,41]. *AANAT* homologs have been cloned from fish [42], humans [31], yeast [43], and mosquitoes [44]. *AANAT* plays a rate-limiting role in melatonin biosynthesis by acetylating serotonin and 5-MT, thus synthesizing *N*-acetylserotonin and melatonin, respectively, in animals and plants [8,36]. An animal *AANAT* homolog was reported in the green alga *C. reinhardtii*, but not in other green algae or higher plants [5]. Okazaki et al. [22] expressed *C. reinhardtii* *AANAT* in *E. coli* and reported that the purified GST-CrAANAT fusion protein transferred an acetyl-CoA group to serotonin but did not determine its  $K_m$  and  $V_{max}$  values. Furthermore, its overexpression in tomato increased melatonin synthesis, but this did not affect the plant phenotype. The  $K_m$  and  $V_{max}$  values of purified recombinant CrAANAT for serotonin indicated that CrAANAT encodes a SNAT enzyme. Similar to other plant SNAT proteins, CrAANAT prefers a high pH, but an optimum temperature of around 37 °C, like animal AANATs [45]. This optimum temperature of CrAANAT is in contrast to that of other plant SNAT enzymes (45 °C to 55 °C) [8], indicating that CrAANAT possesses characteristics of animal AANAT and plant SNAT proteins.

Melatonin has diverse functions in plant growth, development, and biotic and abiotic stress responses [9,10,46–49] by modulating the cellular redox balance [50–52] and protein quality control [53]. Additionally, melatonin functions in concert with other plant hormones during growth and under stressful conditions [54,55]. Melatonin directly influences hormone levels in *Arabidopsis thaliana*, in which exogenous melatonin promotes primary root growth via the indole-3-acetic acid signaling pathway [56]. Indirect effects of melatonin on plant hormones have been reported in plants with up- or down-regulated melatonin synthesis [57,58]. Melatonin did not directly enhance gibberellic acid (GA) synthesis [57] and BR effects such as leaf angle increases [58]. However, melatonin suppression in an *A. thaliana* knockout mutant (*snat1*) and *SNAT2* RNAi rice plants resulted in decreased levels of GA and BR, respectively. This was caused by decreased starch synthesis, which is promoted by melatonin [57,59,60]. An increased endogenous melatonin level in transgenic rice overexpressing caffeic acid *O*-methyltransferase (COMT) markedly increased the seed size and rice yield as a result of elevated cytokinin levels [61]. Transgenic rice plants overexpressing *SNAT* genes from Archaea and rice showed an increase in seed size [62,63]; however, whether this is caused by cytokinins or BRs is unclear. Here, the increased rice seed length caused by an increased endogenous melatonin level was linked to increased BR levels due to upregulation of BR biosynthetic genes (Figure 9), not increased cytokinin levels as in COMT-overexpressing rice [61]. Moreover, the increase in BR levels caused by endogenous melatonin overproduction induces melatonin biosynthesis by activating the expression of melatonin biosynthetic genes such as *tryptophan decarboxylase 1* (*TDC1*), *TDC3*, and *tryptamine 5-hydroxylase* (*T5H*) [64] (Figure 9). In sum, the effect of melatonin on seed size and yield [17,61] and stress tolerance [65,66] suggests that the generation of melatonin-rich rice plants by exogenous application [64] or transgenic approaches [4] would increase yields and resistance to many biotic and abiotic stresses and enable the production of melatonin-rich foods with health benefits [67].

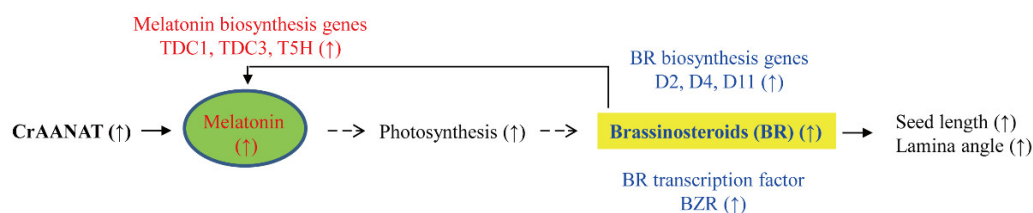


**Figure 9.** Proposed model for the melatonin-mediated increase in seed length. The increase in melatonin synthesis caused by ectopic overexpression of *CrAANAT* leads to an increased seed length and leaf angle, key phenotypic markers of increased BR levels in rice. A number of BR biosynthesis- and signaling-related genes were upregulated in the *CrAANAT*-overexpressing rice plants. These data suggest that melatonin is positively associated with BR levels in rice plants. The melatonin-induced BR increase is an indirect effect on photosynthesis—melatonin is positively coupled to starch synthesis and photosynthesis, which affect BR biosynthesis [57]. BR triggers melatonin biosynthesis by inducing the expression of melatonin biosynthesis genes such as *tryptophan decarboxylase 1 (TDC1)*, *TDC3*, and *tryptamine 5-hydroxylase (T5H)* [64]. Solid arrows, confirmed functions; dashed arrows, steps not yet demonstrated in rice. ↑, upregulation.

## 5. Conclusions

*CrAANAT* had homology to animal AANAT proteins but not to plant SNAT proteins. Its optimum temperature was 37 °C, similar to animal AANAT proteins, but its optimum pH was pH 8.8, similar to plant SNAT proteins, demonstrating that *CrAANAT* has characteristics of both animal AANAT and plant SNAT proteins. Ectopic overexpression of *CrAANAT* in the rice genome led to an increase in melatonin content, leaf angle, and seed length, indicative of enhanced BR biosynthesis. An increased BR level in *CrAANAT*-OE rice plants was indirectly verified by the upregulation of BR biosynthetic genes such as *D2*, *D4*, and *D11*. This is the first report of an increase in BR biosynthesis by the ectopic overexpression of AANAT or SNAT in transgenic plants. Many RNAi transgenic rice plants with downregulated melatonin synthesis show decreased BR levels and leaf angle, suggesting a close relationship between melatonin and BR levels in rice plants [39,61]. The *CrAANAT* can be used as a source gene for a simultaneous increase of melatonin and BR which will lead to improved plant growth and stress tolerance conferred by either melatonin or BR alone or a combination of both [38,39,50].

**Supplementary Materials:** The following supporting information can be downloaded at: <https://www.mdpi.com/article/10.3390/antiox11081531/s1>, Table S1: Sequences of primers used for polymerase chain reaction.

**Author Contributions:** Conceptualization, K.B.; formal analysis, O.-J.H.; investigation, O.-J.H.; K.B.; writing-original draft preparation, K.B.; writing-review and editing, funding acquisition, O.-J.H. All authors have read and agreed to the published version of the manuscript.

**Funding:** This research was supported by the Basic Science Research Program through the National Research Foundation (NRF-2021R1C1C2006271) of the Republic of Korea.

**Institutional Review Board Statement:** Not applicable.

**Informed Consent Statement:** Not applicable.

**Data Availability Statement:** Data presented in this study are available within the article.

**Conflicts of Interest:** The authors declare no conflict of interest.

## References

1. Zhao, D.; Yu, Y.; Shen, Y.; Liu, Q.; Zhao, Z.; Sharma, R.; Reiter, R.J. Melatonin synthesis and function: Evolutionary history in animals and plants. *Front. Endocrinol.* **2019**, *10*, 249. [CrossRef]
2. Back, K. Melatonin metabolism, signaling and possible roles in plants. *Plant J.* **2021**, *105*, 376–391. [CrossRef] [PubMed]
3. Coon, S.L.; Klein, D.C. Evolution of arylalkylamine *N*-acetyltransferase: Emergence and divergence. *Mol. Cell. Endocrinol.* **2006**, *252*, 2–10. [CrossRef] [PubMed]

4. Liao, L.; Zhou, Y.; Xu, Y.; Zhang, Y.; Liu, X.; Liu, B.; Chen, X.; Guo, Y.; Zeng, Z.; Zhao, Y. Structural and molecular dynamics analysis of plant serotonin *N*-acetyltransferase reveal an acid/base-assisted catalysis in melatonin biosynthesis. *Angew. Chem Int. Ed.* **2021**, *60*, 12020–12026. [[CrossRef](#)]
5. Sasso, S.; Stibor, H.; Mittag, M.; Grossman, A.R. From molecular manipulation of domesticated *Chlamydomonas reinhardtii* to survival in nature. *eLife* **2018**, *7*, e39233. [[CrossRef](#)] [[PubMed](#)]
6. Merchant, S.S.; Prochnik, S.E.; Vallon, O.; Harris, E.H.; Karpowicz, S.J.; Witman, G.B.; Terry, A.; Salamov, A.; Fritz-Laylin, L.K.; Maréchal-Drouard, L.; et al. The *Chlamydomonas* genome reveals the evolution of key animal and plant functions. *Science* **2007**, *318*, 245–250. [[CrossRef](#)]
7. Voisin, P.; Namboodiri, M.A.; Klein, D.C. Arylamine *N*-acetyltransferase and arylalkylamine *N*-acetyltransferase in the mammalian pineal gland. *J. Biol. Chem.* **1984**, *259*, 10913–10918. [[CrossRef](#)]
8. Lee, H.Y.; Hwang, O.J.; Back, K. Functional characterization of tobacco (*Nicotiana benthamiana*) serotonin *N*-acetyltransferases (*NbSNAT1* and *NbSNAT2*). *Melatonin Res.* **2021**, *4*, 507–521.
9. Sun, C.; Liu, L.; Wang, L.; Li, B.; Jin, C.; Lin, X. Melatonin: A master regulator of plant development and stress responses. *J. Integr. Plant Biol.* **2021**, *63*, 126–145. [[CrossRef](#)]
10. Arnao, M.B.; Cano, A.; Hernández-Ruiz, J. Phytomelatonin: An unexpected molecule with amazing performance in plants. *J. Exp. Bot.* **2022**. [[CrossRef](#)]
11. Yao, J.W.; Ma, Z.; Ma, Y.Q.; Zhu, Y.; Lei, M.Q.; Hao, C.Y.; Chen, L.Y.; Xu, Z.Q.; Huang, X. Role of melatonin in UV-B signaling pathway and UV-B stress resistance in *Arabidopsis thaliana*. *Plant Cell Environ.* **2021**, *44*, 114–129. [[CrossRef](#)] [[PubMed](#)]
12. Wang, X.; Zhang, H.; Xie, Q.; Liu, Y.; Lv, H.; Bai, R.; Ma, R.; Li, X.; Zhang, X.; Guo, Y.D.; et al. SISNAT interacts with HSP40, a molecular chaperone, to regulate melatonin biosynthesis and promote thermotolerance in tomato. *Plant Cell Physiol.* **2020**, *61*, 909–921. [[CrossRef](#)] [[PubMed](#)]
13. Yu, Y.; Bian, L.; Jiao, Z.; Keke, Y.; Wan, Y.; Zhang, G.; Guo, D. Molecular cloning and characterization of a grapevine (*Vitis vinifera* L.) serotonin *N*-acetyltransferase (*VvSNAT2*) gene involved in plant defense. *BMC Genom.* **2019**, *20*, 880. [[CrossRef](#)]
14. Zhao, G.; Yu, X.; Lou, W.; Wei, S.; Wang, R.; Wan, Q.; Shen, W. Transgenic Arabidopsis overexpressing *MsSNAT* enhances salt tolerance via the increase in autophagy, and the reestablishment of redox and ion homeostasis. *Environ. Exp. Bot.* **2019**, *164*, 20–28. [[CrossRef](#)]
15. Lee, H.Y.; Back, K. Melatonin induction and its role in high light stress tolerance in *Arabidopsis thaliana*. *J. Pineal Res.* **2018**, *65*, e12504. [[CrossRef](#)]
16. Gu, Q.; Chen, Z.; Yu, X.; Cui, W.; Pan, J.; Zhao, G.; Xu, S.; Wang, R.; Shen, W. Melatonin confers plant tolerance against cadmium stress via the decrease of cadmium accumulation and reestablishment of microRNA-mediated redox homeostasis. *Plant Sci.* **2017**, *261*, 28–37. [[CrossRef](#)]
17. Lee, K.; Back, K. Overexpression of rice serotonin *N*-acetyltransferase 1 in transgenic rice plants confers resistance to cadmium and senescence and increases grain yield. *J. Pineal Res.* **2017**, *62*, e12392. [[CrossRef](#)]
18. Wang, L.; Zhao, Y.; Reiter, R.J.; He, C.; Liu, G.; Lei, Q.; Zuo, B.; Zheng, X.D.; Li, Q.; Kong, J. Change in melatonin levels in transgenic ‘Micro-Tom’ tomato over-expressing ovine *AANAT* and ovine *HIOMT* genes. *J. Pineal Res.* **2014**, *56*, 134–142. [[CrossRef](#)] [[PubMed](#)]
19. Park, S.; Lee, D.E.; Jang, H.; Byeon, Y.; Kim, Y.S.; Back, K. Melatonin-rich transgenic rice plants exhibit resistance to herbicide-induced oxidative stress. *J. Pineal Res.* **2013**, *54*, 258–263. [[CrossRef](#)]
20. Kang, K.; Lee, K.; Park, S.; Kim, Y.S.; Back, K. Enhanced production of melatonin by ectopic overexpression of human serotonin *N*-acetyltransferase plays a role in cold resistance in transgenic rice seedlings. *J. Pineal Res.* **2010**, *49*, 176–182. [[CrossRef](#)]
21. Tan, D.X.; Manchester, L.C.; Terron, M.P.; Flores, L.J.; Reiter, R.J. One molecule, many derivatives: A never-ending interaction of melatonin with reactive oxygen and nitrogen species? *J. Pineal Res.* **2007**, *42*, 28–42. [[CrossRef](#)] [[PubMed](#)]
22. Okazaki, M.; Higuchi, K.; Hahawa, Y.; Shiraiwa, Y.; Ezura, H. Cloning and characterization of a *Chlamydomonas reinhardtii* cDNA arylalkylamine *N*-acetyltransferase and its use in the genetic engineering of melatonin content in the Micro-Tom tomato. *J. Pineal Res.* **2009**, *46*, 373–382. [[CrossRef](#)] [[PubMed](#)]
23. Byeon, Y.; Lee, H.Y.; Back, K. Cloning and characterization of the serotonin *N*-acetyltransferase-2 gene (*SNAT2*) in rice (*Oryza sativa*). *J. Pineal Res.* **2016**, *61*, 198–207. [[CrossRef](#)] [[PubMed](#)]
24. Byeon, Y.; Lee, H.Y.; Lee, K.; Park, S.; Back, K. Cellular localization and kinetics of the rice melatonin biosynthetic enzymes *SNAT* and *ASMT*. *J. Pineal Res.* **2014**, *56*, 107–114. [[CrossRef](#)]
25. Himmelbach, A.; Zierold, U.; Hensel, G.; Riechen, J.; Douchkov, D.; Schweizer, P.; Kumlehn, J. A set of modular binary vectors for transformation of cereals. *Plant Physiol.* **2007**, *145*, 1192–1200. [[CrossRef](#)]
26. Lee, H.J.; Lee, S.B.; Chung, J.S.; Han, S.U.; Han, O.; Guh, J.O.; Jeon, J.S.; An, G.; Back, K. Transgenic rice plants expressing a *Bacillus subtilis* protoporphyrinogen oxidase gene are resistant to diphenyl ether herbicide oxyfluorfen. *Plant Cell Physiol.* **2000**, *41*, 743–749. [[CrossRef](#)]
27. Lee, K.; Choi, G.H.; Back, K. Cadmium-induced melatonin synthesis in rice requires light, hydrogen peroxide, and nitric oxide: Key regulatory roles for tryptophan decarboxylase and caffeic acid *O*-methyltransferase. *J. Pineal Res.* **2017**, *63*, e12441. [[CrossRef](#)]
28. Kang, K.; Lee, K.; Park, S.; Byeon, Y.; Back, K. Molecular cloning of rice serotonin *N*-acetyltransferase, the penultimate gene in plant melatonin biosynthesis. *J. Pineal Res.* **2013**, *55*, 7–13. [[CrossRef](#)]

29. Lee, H.Y.; Lee, K.; Back, K. Knockout of *Arabidopsis* serotonin *N*-acetyltransferase-2 reduces melatonin levels and delays flowering. *Biomolecules* **2019**, *9*, 712. [[CrossRef](#)]
30. De Angelis, J.; Gastel, J.; Klein, D.C.; Cole, P.A. Kinetic analysis of the catalytic mechanism of serotonin *N*-acetyltransferase (EC 2.3.1.87). *J. Biol. Chem.* **1998**, *273*, 3045–3050. [[CrossRef](#)]
31. Ferry, G.; Loynel, A.; Kucharczyk, N.; Bertin, S.; Rodriguez, M.; Delagrangé, P.; Galizzi, J.-P.; Jacoby, E.; Volland, J.-P.; Lesieur, D.; et al. Substrate specificity and inhibition studies of human serotonin *N*-acetyltransferase. *J. Biol. Chem.* **2000**, *275*, 8794–8805. [[CrossRef](#)]
32. Byeon, Y.; Lee, H.Y.; Choi, D.W.; Back, K. Chloroplast encoded serotonin *N*-acetyltransferase in the red alga *Pyropia yezoensis*: Gene transition to the nucleus from chloroplasts. *J. Exp. Bot.* **2015**, *66*, 709–717. [[CrossRef](#)]
33. Byeon, Y.; Lee, K.; Park, Y.I.; Park, S.; Back, K. Molecular cloning and functional analysis of serotonin *N*-acetyltransferase from the cyanobacterium *Synechocystis* sp. PCC 6803. *J. Pineal Res.* **2013**, *55*, 371–376. [[CrossRef](#)] [[PubMed](#)]
34. Emanuelsson, O.; Nielsen, H.; Brunak, S.; Heijne, G. Predicting subcellular localization of proteins based on their N-terminal amino acid sequence. *J. Mol. Biol.* **2000**, *300*, 1005–1016. [[CrossRef](#)] [[PubMed](#)]
35. Byeon, Y.; Lee, H.Y.; Lee, K.; Back, K. A rice chloroplast transit peptide sequence does not alter the cytoplasmic localization of sheep serotonin *N*-acetyltransferase expressed in transgenic rice plants. *J. Pineal Res.* **2014**, *57*, 147–154. [[CrossRef](#)] [[PubMed](#)]
36. Tan, D.X.; Hardeland, R.; Back, K.; Manchester, L.C.; Alatorre-Jimenez, M.A.; Reiter, R.J. On the significance of an alternate pathway of melatonin synthesis via 5-methoxytryptamine: Comparisons across species. *J. Pineal Res.* **2016**, *61*, 27–40. [[CrossRef](#)]
37. Jiang, H.; Zhang, A.; Liu, X.; Chen, J. Grain size associated genes and the molecular regulatory mechanism in rice. *Int. J. Mol. Sci.* **2022**, *23*, 3169. [[CrossRef](#)]
38. Zhang, C.; Bai, M.; Chong, K. Brassinosteroid-mediated regulation of agronomic traits in rice. *Plant Cell Rep.* **2014**, *33*, 683–696. [[CrossRef](#)]
39. Hwang, H.; Ryu, H.; Cho, H. Brassinosteroid signaling pathways interplaying with diverse signaling cues for crop enhancement. *Agronomy* **2022**, *11*, 556. [[CrossRef](#)]
40. Coon, S.L.; Roseboom, P.H.; Baler, R.; Weller, J.L.; Nambroodiri, M.A.A.; Koonin, E.V.; Klein, D.C. Pineal serotonin *N*-acetyltransferase: Expression cloning and molecular analysis. *Science* **1995**, *270*, 1681–1683. [[CrossRef](#)]
41. Borjigin, J.; Wang, M.M.; Snyder, S.H. Diurnal variation in mRNA encoding serotonin *N*-acetyltransferase in pineal gland. *Nature* **1995**, *378*, 783–785. [[CrossRef](#)] [[PubMed](#)]
42. Coon, S.L.; Bégay, V.; Deurloo, D.; Falcón, J.; Klein, D.C. Two arylalkylamine *N*-acetyltransferase genes mediate melatonin synthesis in fish. *J. Biol. Chem.* **1999**, *274*, 9076–9082. [[CrossRef](#)] [[PubMed](#)]
43. Ganguly, S.; Mummaneni, P.; Steinbach, P.J.; Klein, D.C.; Coon, S.L. Characterization of the *Saccharomyces cerevisiae* homolog of the melatonin rhythm enzyme arylalkylamine *N*-acetyltransferase (EC 2.3.1.87). *J. Biol. Chem.* **2001**, *276*, 47239–47247. [[CrossRef](#)]
44. Mehere, P.; Han, Q.; Christensen, B.M.; Li, J. Identification and characterization of two arylalkylamine *N*-acetyltransferases in the yellow fever mosquito, *Aedes aegypti*. *Insect Biochem. Mol. Biol.* **2011**, *41*, 707–714. [[CrossRef](#)] [[PubMed](#)]
45. Zhan-Poe, X.; Craft, C.M. Biochemical characterization of recombinant serotonin *N*-acetyltransferase. *J. Pineal Res.* **1999**, *27*, 49–58. [[CrossRef](#)] [[PubMed](#)]
46. Ahmad, S.; Wang, G.Y.; Muhammad, I.; Chi, Y.X.; Zeeshan, M.; Nasar, J.; Zhou, X.B. Interactive effects of melatonin and nitrogen improve drought tolerance of maize seedlings by regulating growth and physiological attributes. *Antioxidants* **2022**, *11*, 359. [[CrossRef](#)] [[PubMed](#)]
47. Ali, M.; Lamin-Samu, A.T.; Muhammad, I.; Farghal, M.; Khattak, A.M.; Jan, I.; Haq, S.U.; Khan, A.; Gong, Z.-H.; Lu, G. Melatonin mitigates the infection of *Colletotrichum gloeosporioides* via modulation of the chitinase gene and antioxidant activity in *Capsicum annuum* L. *Antioxidants* **2021**, *10*, 7. [[CrossRef](#)]
48. Bhardwaj, R.; Pareek, S.; Domínguez-Avila, J.A.; Gonzalez-Aguilar, G.A.; Valero, D.; Serrano, M. An exogenous pre-storage melatonin alleviates chilling injury in some mango fruit cultivars, by acting on the enzymatic and non-enzymatic antioxidant system. *Antioxidants* **2022**, *11*, 384. [[CrossRef](#)]
49. Jiang, Y.; Huang, S.; Ma, L.; Kong, L.; Pan, S.; Tang, X.; Tian, H.; Duan, M.; Mo, Z. Effects of exogenous melatonin application on the grain yield and antioxidant capacity in aromatic rice under combined lead-cadmium stress. *Antioxidants* **2022**, *11*, 776. [[CrossRef](#)]
50. Zhao, D.; Wang, H.; Chen, S.; Yu, D.; Reiter, R.J. Phytomelatonin: An emerging regulator of plant biotic stress resistance. *Trends Plant Sci.* **2021**, *26*, 70–82. [[CrossRef](#)]
51. Pardo-Hernández, M.; López-Delacalle, M.; Rivero, R.M. ROS and NO regulation by melatonin under abiotic stress in plants. *Antioxidants* **2020**, *9*, 1078. [[CrossRef](#)] [[PubMed](#)]
52. Zhang, T.; Wang, Y.; Ma, X.; Ouyang, Z.; Deng, L.; Shen, S.; Dong, X.; Du, N.; Dong, H.; Guo, Z.; et al. Melatonin alleviates copper toxicity via improving ROS metabolism and antioxidant defense response in tomato seedlings. *Antioxidants* **2022**, *11*, 758. [[CrossRef](#)] [[PubMed](#)]
53. Lee, H.Y.; Hwang, O.J.; Back, K. Phytomelatonin as a signaling molecule for protein quality control via chaperone, autophagy, and ubiquitin–proteasome systems in plants. *J. Exp. Bot.* **2022**. [[CrossRef](#)] [[PubMed](#)]
54. Arnao, M.B.; Hernández-Ruiz, J. Melatonin and its relationship to plant hormones. *Ann. Bot.* **2018**, *121*, 195–207. [[CrossRef](#)]
55. Yang, X.; Chen, J.; Ma, Y.; Huang, M.; Qiu, T.; Bian, H.; Han, N.; Wang, J. Function, mechanism, and application of plant melatonin: An update with a focus on the cereal crop, barley (*Hordeum vulgare* L.). *Antioxidants* **2022**, *11*, 634. [[CrossRef](#)] [[PubMed](#)]

56. Yang, L.; You, J.; Li, J.; Wang, Y.; Chan, Z. Melatonin promotes Arabidopsis primary root growth in an IAA-dependent manner. *J. Exp. Bot.* **2021**, *72*, 5599–5611. [[CrossRef](#)]
57. Lee, H.Y.; Back, K. Melatonin regulates chloroplast protein quality control via a mitogen-activated protein kinase signaling pathway. *Antioxidants* **2021**, *10*, 511. [[CrossRef](#)]
58. Hwang, O.J.; Back, K. Melatonin is involved in skotomorphogenesis by regulating brassinosteroid biosynthesis in plants. *J. Pineal Res.* **2018**, *65*, e12495. [[CrossRef](#)]
59. Altaf, M.A.; Shahid, R.; Ren, M.X.; Naz, S.; Altaf, M.M.; Khan, L.U.; Tiwari, R.K.; Lal, M.K.; Shahid, M.A.; Kumar, R.; et al. Melatonin improves drought tolerance of tomato by modulating plant growth, root architecture, photosynthesis, and antioxidant defense system. *Antioxidants* **2022**, *11*, 309. [[CrossRef](#)]
60. Muhammad, I.; Yang, L.; Ahmad, S.; Mosaad, I.S.M.; Al-Ghamdi, A.A.; Abbasi, A.M.; Zhou, X.-B. Melatonin application alleviates stress-induced photosynthetic inhibition and oxidative damage by regulating antioxidant defense system of maize: A meta-analysis. *Antioxidants* **2022**, *11*, 512. [[CrossRef](#)]
61. Huangfu, L.; Chen, R.; Lu, Y.; Zhang, E.; Miao, J.; Zuo, Z.; Zhao, Y.; Zhu, M.; Zhang, Z.; Li, P.; et al. *OsCOMT*, encoding a caffeic acid O-methyltransferase in melatonin biosynthesis, increases rice grain yield through dual regulation of leaf senescence and vascular development. *Plant Biotechnol. J.* **2022**, *20*, 1122–1139. [[CrossRef](#)] [[PubMed](#)]
62. Hwang, O.J.; Back, K. Melatonin deficiency confers tolerance to multiple abiotic stresses in rice via decreased brassinosteroid levels. *Int. J. Mol. Sci.* **2019**, *20*, 5173. [[CrossRef](#)] [[PubMed](#)]
63. Lee, K.; Choi, G.H.; Back, K. Functional characterization of serotonin *N*-acetyltransferase in archaeon *Thermoplasma volcanium*. *Antioxidants* **2022**, *11*, 596. [[CrossRef](#)] [[PubMed](#)]
64. Hwang, O.J.; Back, K. Molecular regulation of antioxidant melatonin biosynthesis by brassinosteroid acting as an endogenous elicitor of melatonin induction in rice seedling. *Antioxidant* **2022**, *11*, 918. [[CrossRef](#)] [[PubMed](#)]
65. Sharma, A.; Zheng, B. Melatonin mediated regulation of drought stress: Physiological and molecular aspects. *Plants* **2019**, *8*, 190. [[CrossRef](#)] [[PubMed](#)]
66. Li, R.; Yang, R.; Zheng, W.; Wu, L.; Zhang, C.; Zhang, H. Melatonin promotes SGT1involved signals to ameliorate drought stress adaption in rice. *Int. J. Mol. Sci.* **2022**, *23*, 599. [[CrossRef](#)]
67. Kuwabara, W.M.T.; Gomes, P.R.L.; Andrade-Silva, J.; Soares, J.M., Jr.; Amaral, F.G.; Cipolla-Neto, J. Melatonin and its ubiquitous effects on cell function and survival: A review. *Melatonin Res.* **2022**, *5*, 192–208. [[CrossRef](#)]